to the fast codes (NMSERS, PATRN1). The DSDA was about as fast, or faster than, any code solving Problems 3, 5, and 6 and was significantly faster than average in all others except Problem 9 where it was about average in speed. Compared to the relatively reliable codes ($n_s \leq 8$) the DSDA was faster than PATSH on six of eight problems that both codes solved, faster than SEEK3 in six of seven problems and faster than SIMPLX in all problems solved by both schemes. Thus on the basis of this comparison the DSDA appears to be a superior nonlinear MP code.

It may be seen that the gradient based procedures, including those employing the SUMT strategy and penalty function,[8] so widely used in engineering problems, performed rather poorly. The best gradient based code DAVID solved only half the problems. The direct search procedures in general provided much better performance although only two, the DSDA and PATSH, solved, or approached the solution to, all ten problems.

It should be noted, however, that this comparison employed rather small test problems (two to five variables with zero to ten behavior constraints). It is not clear that the direct search procedures would also possess reliability and speed superior to the gradient methods on large problems. Still the superiority in this study of the better direct search procedures is dramatic while the performance of the gradient schemes is rather dismal. The unreliability of the popular gradient schemes is particularly disturbing since these schemes performed best on those problems without any active behavior constraints (problems 4, 5, and 8). No gradient scheme solved half or more of the problems where a constraint is active at the optimum. Furthermore, although the better direct search procedures may not be as reliable on larger problems one would certainly not expect the reliability of the gradient procedures to improve.

Conclusion

Although it is recognized that such favorable findings on the DSDA code presented by its developer can be viewed with some scepticism, it should be noted that the performance cited is based on rating schemes and problems selected by Eason and Fenton and not by the author, and that this performance was achieved with a conscious effort to avoid any tuning of the code to individual problems. Thus these results indicate that the DSDA appears to be a superior nonlinear mathematical programing procedure at least on relatively small problems. It must be stated, however, that the comparison study cannot be considered sufficiently thorough to make specific claims on the relative superiority of the better direct search procedures.

References

[1] Pappas, M. and Amba-Rao, C. L., "A Direct Search Algorithm for Automated Optimum Structural Design," *AIAA Journal*, Vol. 9, March 1971, pp. 387–393.

[2] Pappas, M. and Amba-Rao, C. L., "Structural Synthesis of Thin Cylindrical Shells with Spiral-Type Stiffeners," *AIAA Journal*, Vol. 8, Aug. 1970, pp. 1529–1530.

[3] Pappas, M. and Allentuch, A., "Structural Synthesis of Frame Reinforced, Submersible, Circular Cylindrical Hulls," *Computers and Structures*, Vol. 4, Jan. 1974, pp. 253–280.

[4] Pappas, M. and Allentuch, A., "Mathematical Programming Procedures for Mixed Discrete-Continuous Design Problems," *Transactions of the Asme, Ser. B: Journal of Engineering for Industry*, Vol. 96, Feb. 1974, pp. 201–209.

[5] Eason, E. D. and Fenton, R. G., "A Comparison of Numerical Optimization Methods for Engineering Design," *Transactions of the ASME, Ser. B: Journal of Engineering for Industry*, Vol. 96, Feb. 1974, pp. 196–200.

[6] Pappas, M., "Use of Direct Search in Automated Optimal Design," *Transactions of the ASME, Ser. B: Journal of Engineering for Industry*, Vol. 94, May 1972, pp. 395–401.

[7] Eason, E. D. and Fenton, R. G., "Testing and Evaluation of Numerical Methods for Design Optimization," Rept. UTME-TP 7204, Sept. 1972, Technical Publication Series, Dept. of Mech. Eng., Univ. of Toronto, Toronto, Canada.

[8] Fracco, A. V. and McCormick, G. P., *Nonlinear Programming: Sequential Unconstrained Minimization Techniques*, Wiley, New York, 1968.

Boundary Layers on a Rotating Disk

TUNCER CEBECI*
California State University, Long Beach, Calif.

AND

DOUGLAS E. ABBOTT†
Purdue University, Lafayette, Ind.

Nomenclature

A	= damping-length constant
c_{f_θ}	= circumferential local skin-friction coefficient
f	= radial stream function
g	= circumferential stream function
r	= radial coordinate (radius from axis of rotation)
R_r	= rotational Reynolds number, $\omega r^2/\nu$
R_θ	= Reynolds number based on momentum thickness, $\theta\omega r/\nu$
u, v, w	= mean radial, axial, and circumferential velocity components, respectively
y	= axial coordinate = distance perpendicular to the disk
γ_{tr}	= intermittency factor
ε	= eddy viscosity
ε^+	= dimensionless eddy viscosity, ε/ν
η	= similarity parameter
θ	= momentum thickness, $\theta = \int_0^\infty w/\omega r(1 - w/\omega r)\,dy$
μ	= dynamic viscosity
ν	= kinematic viscosity = μ/ρ
ρ	= density
τ	= shear stress
ω	= angular velocity of disk

Subscripts

i	= inner region
o	= outer region
w	= wall

Primes denote differentiation with respect to η

Introduction

A DISK rotating in an infinite quiescent fluid is one of the simplest types of three-dimensional boundary-layer flow. Depending on the Reynolds number based on radius and angular velocity, we may have laminar, transitional, and turbulent boundary layers. According to experiments,[1] the flow is laminar if the Reynolds number is less than approximately 1.85×10^5. The flow is transitional for Reynolds number between 1.85×10^5 and 2.85×10^5. It is fully turbulent for Reynolds number greater than 2.85×10^5.

In this Note, we discuss the prediction of laminar, transitional, and turbulent boundary layers on a rotating disk by an efficient numerical method. The method employs the eddy viscosity concept to model the Reynolds shear stress terms and has been previously used to compute two-dimensional boundary layers[2] and recently three-dimensional boundary layers.[3,4] Results are

Received October 2, 1974; revision received December 12, 1974. This work was supported by the National Science Foundation Grant No. ENG74-11895.

Index categories: Boundary Layers and Convective Heat Transfer—Turbulent.

* Adjunct Professor, Mechanical Engineering Department. Member AIAA.

† Professor, Mechanical Engineering Department.

given for values of the rotational Reynolds number from zero to 2×10^6.

Basic Equations

The boundary-layer equations for steady incompressible three-dimensional, axisymmetric flow near the rotating disk in the absence of a radial pressure gradient are:

Continuity

$$\frac{1}{r}\frac{\partial}{\partial r}(ur) + \frac{\partial v}{\partial y} = 0 \tag{1}$$

Momentum in the radial direction

$$u\frac{\partial u}{\partial r} + v\frac{\partial u}{\partial y} - \frac{w^2}{r} = \frac{1}{\rho}\frac{\partial}{\partial y}\left(\mu\frac{\partial u}{\partial y} - \rho\overline{u'v'}\right) \tag{2}$$

Momentum in the circumferential direction

$$u\frac{\partial w}{\partial r} + v\frac{\partial w}{\partial y} + \frac{uw}{r} = \frac{1}{\rho}\frac{\partial}{\partial y}\left(\mu\frac{\partial w}{\partial y} - \rho\overline{v'w'}\right) \tag{3}$$

These equations are subject to the boundary conditions:

$$y = 0 \qquad u = 0 \qquad w = \omega r \tag{4a}$$

$$y \to \infty \qquad u = 0 \qquad w = 0 \tag{4b}$$

Before we solve system (1–3), we first transform it by using the similarity variable

$$\eta = (\omega/\nu)^{1/2} y \tag{5a}$$

and introduce the dimensionless stream function $f(r, \eta)$ defined by

$$\psi(r, y) = (\nu\omega)^{1/2} r^2 f(r, \eta) \tag{5b}$$

where $ur = (\partial\psi/\partial y)$, and $vr = -(\partial\psi/\partial r)$. With the concept of eddy viscosity, the Reynolds shear stress terms in Eqs. (2) and (3) can be written as

$$-\rho\overline{u'v'} = \rho\varepsilon(\partial u/\partial y), \qquad -\rho\overline{v'w'} = \rho\varepsilon(\partial w/\partial y) \tag{6}$$

With Eqs. (5) and (6), system (1–3) can be written as

Momentum equation in the radial direction

$$[(1+\varepsilon^+)f'']' + 2ff'' - (f')^2 + (g')^2 = r\left(f'\frac{\partial f'}{\partial r} - f''\frac{\partial f}{\partial r}\right) \tag{7}$$

Momentum equation in the circumferential direction

$$[(1+\varepsilon^+)g'']' + 2fg'' - 2f'g' = r\left(f'\frac{\partial g'}{\partial r} - g''\frac{\partial f}{\partial r}\right) \tag{8}$$

Here primes denote differentiation with respect to η and

$$\varepsilon^+ = \varepsilon/\nu, \qquad f' = (u/u_r), \qquad g' = (w/u_r), \qquad u_r = \omega r \tag{9}$$

The boundary conditions (4) become

$$\eta = 0 \qquad f' = 0 \qquad g' = 1 \tag{10a}$$

$$\eta \to \infty \qquad f' = 0 \qquad g' = 0 \tag{10b}$$

Eddy-Viscosity Formulation

At present, there are several mixing-length and eddy-viscosity formulations being used to model the Reynolds shear-stress terms in the boundary-layer equations. Here we shall use the one developed by Cebeci and Smith.[2] This formulation accounts for various boundary-layer effects such as high and low Reynolds numbers, transitional flows, mass transfer, etc., and has been shown to give good results.[2] It has also been extended to three-dimensional boundary layers, again producing good results.[3,4] The extension of this formulation to a rotating disk is presented.

Because of the composite nature of a turbulent boundary layer, we divide the layer into inner and outer regions and define corresponding eddy viscosity formulas by separate expressions in each region. In the inner region of the boundary layer, we define the inner eddy-viscosity by

$$\varepsilon_i = L^2\left[\left(\frac{\partial u}{\partial y}\right)^2 + \left(\frac{\partial \bar{w}}{\partial y}\right)^2\right]^{1/2} \tag{11}$$

where

$$L = \kappa y[1 - \exp(-y/A)] \tag{12a}$$

$$\bar{w} = \omega x - w \tag{12b}$$

In Eq. (12a), κ is von Kármán's constant equal to 0.40 and A is a damping-length parameter given by

$$A = A^+\nu\left(\frac{\tau_w}{\rho}\right)^{-1/2} \tag{12c}$$

with $A^+ = 26$. In the outer region of the boundary layer, we define the outer eddy viscosity by

$$\varepsilon_o = \alpha\left|\int_0^\infty [\omega x - (u^2 + \bar{w}^2)^{1/2}]\right| dy \tag{13}$$

where α is a "universal" constant equal to 0.0168.

To account for the effect of low Reynolds number and to account for the transitional region between a laminar and turbulent boundary, we modify the expressions given by Eqs. (11–13). To account for the low Reynolds number effect, we use the expressions given by Cebeci and Mosinskis[5] and by Cebeci.[6] According to Ref. 5, κ and A^+ are functions of Reynolds number given by

$$\kappa = 0.40 + 0.19/(1 + 0.19 z_2{}^2) \tag{14a}$$

and

$$A^+ = 26 + 14/(1 + z_2{}^2) \tag{14b}$$

where $z_2 = R_\theta \times 10^{-3} > 0.3$. According to Ref. 6, α is a function of Reynolds number given by

$$\alpha = 0.0168[1.55/(1 + \Pi)] \tag{15a}$$

where

$$\Pi = 0.55[1 - \exp(-0.243 z_1{}^{1/2} - 0.298 z_1)] \tag{15b}$$

and $z_1 = (R_\theta/425 - 1)$.

As previously discussed, the flow is fully turbulent when the rotational Reynolds number is greater than 2.85×10^5; for the range of 1.85×10^5 and 2.85×10^5, the flow is transitional. The eddy viscosity formulation given by Eqs. (11–15) is based on experimental data obtained for fully turbulent flows. For this reason, the formulation should not be used to compute transitional boundary layers unless it is corrected for the intermittent behavior of the boundary layer in the transitional region.[7] In the eddy-viscosity methods, the "correction" is usually made by multiplying the inner and outer eddy-viscosity formulas by an intermittency factor. Several authors have tried this approach and have obtained satisfactory agreement with experiment. According to the expression used by Cebeci,[8] the intermittency factor for an incompressible turbulent boundary layer with zero pressure gradient is given by

$$\gamma_{tr} = 1 - \exp[-G(x - x_{tr})^2] \tag{16a}$$

where

$$G = 0.835 \times 10^{-3}(u_e{}^2/\nu^2) R_{x_{tr}}^{-1.34}, \qquad R_x = (u_e x/\nu) \tag{16b}$$

By interpreting R_x as a rotational Reynolds number, $R_r \equiv \omega r^2/\nu$, and taking $u_e = \omega r$, we may write Eq. (16) as

$$\gamma_{tr} = 1 - \exp[-G(r - r_{tr})^2] \tag{17a}$$

and

$$G = 0.835 \times 10^{-3}\left(\frac{R_r}{r}\right)^2 R_{r_{tr}}^{-1.34} \tag{17b}$$

In transformed coordinates, it can be shown that the inner and outer eddy viscosity formulas can be written as

$$\varepsilon_i{}^+ = (\kappa\eta)^2 R_r{}^{1/2}\left[1 - \exp\left(-R_r{}^{-1/2}\eta\frac{r}{A}\right)\right]^2 \times [(f'')^2 + (g'')^2]^{1/2}\gamma_{tr} \qquad \varepsilon_i{}^+ \leq \varepsilon_o{}^+ \tag{18a}$$

$$\varepsilon_o{}^+ = \alpha R_r{}^{1/2}\left|\int_0^\infty \{1 - [(f')^2 + (1 - g')^2]^{1/2}\} d\eta\right| \gamma_{tr} \tag{18b}$$

Here

$$A = \frac{A^+ r}{R_r{}^{3/4}[(f_w'')^2 + (g_w'')^2]^{1/4}} \tag{19}$$

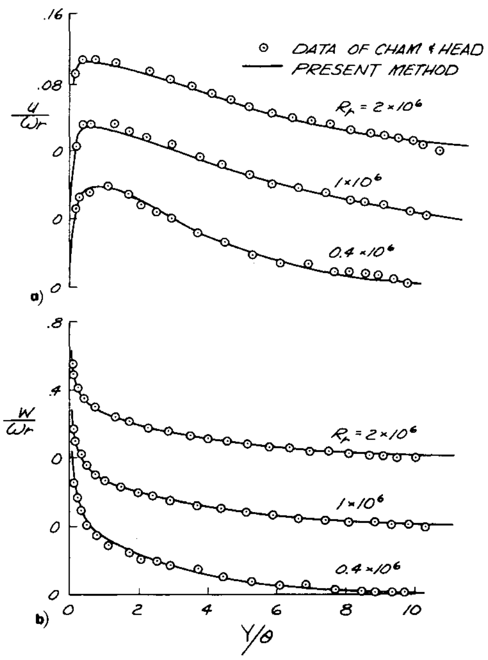

Fig. 1 Comparison of turbulent mean, a) radial and b) circumferential velocity profiles.

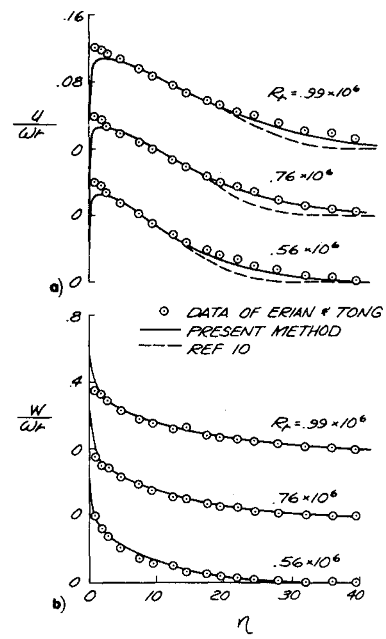

Fig. 3 Comparison of turbulent mean, a) radial and b) circumferential velocity profiles.

and κ, A^+, α, and γ_{tr} are given by Eqs. (14a, 14b, 15, and 17), respectively. Equations (18) are then the eddy viscosity formulation used in the present paper.

Comparison with Experiment

We have used the numerical method of H. B. Keller,[9] described in Ref. 3 to solve the system given by Eqs. (7, 8, 10, 18). After writing the basic equations (7) and (8) as a first-order system the derivatives are approximated by centered difference quotients and averages centered at the midpoints of net rectangles or net segments. Arbitrary (nonuniform) meshes are used and second-order accuracy is retained. The nonlinear difference equations are solved by Newton's method using an efficient block-tridiagonal factorization technique. For details, see Refs. 2, 3, and 9.

Figures 1–3 show the results obtained by our method. Figure 1 shows the mean radial and circumferential velocity profiles for a turbulent flow. The calculations were started as laminar at $r = 0$, and were continued as laminar until $R_r = 1.85 \times 10^5$. At that location, the turbulent flow calculations were started by activating the eddy-viscosity formulas in the solution of the governing equations.

Figure 2 shows the comparison of calculated and experimental circumferential skin-friction coefficient c_{f_θ} defined by

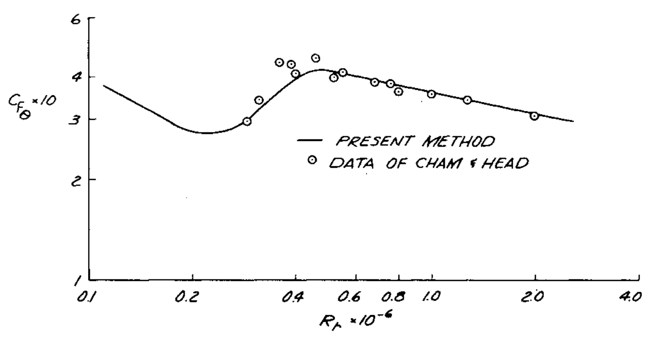

Fig. 2 Comparison of circumferential skin-friction component.

$$c_{f_\theta} = \frac{2\mu}{\rho\omega^2 r^2}\left(\frac{\partial w}{\partial y}\right)_w \tag{20a}$$

which in terms of transformed variables can be written as

$$c_{f_\theta} = (2/r)(v/\omega)^{1/2} g_w'' \tag{20b}$$

The agreement with measured velocity profiles and skin friction is very satisfactory.

Figure 3 shows a comparison of calculated and experimental turbulent mean radial and circumferential velocity profiles. The data is due to Erian and Tong.[11] Shown in the plots are the predictions of Ref. 10, which was obtained by a different extension of the Cebeci-Smith eddy-viscosity formulation.[2] Again our results agree well with the experimental data.

In conclusion, the method presented here for predicting the three-dimensional boundary layer that develops on a rotating disk is found to be in good agreement with the available experimental data. The method accounts for complete flows, including laminar, transitional, and turbulent regions. The method is capable of accurate predictions of detailed velocity profiles as well as the conventional boundary-layer parameters.

References

[1] Cham, T. S. and Head, M. R., "Turbulent Boundary-Layer Flow on a Rotating Disk," *Journal of Fluid Mechanics*, Vol. 37, Pt. 1, June 1969, pp. 129–147.

[2] Cebeci, T. and Smith, A. M. O., *Analysis of Turbulent Boundary Layers*, Academic Press, New York, 1974.

[3] Cebeci, T., "Calculation of Three-Dimensional Boundary Layers, I. Swept Infinite Cylinders and Small Cross Flow," *AIAA Journal*, Vol. 12, June 1974, pp. 779–786.

[4] Cebeci, T., "Calculation of Three-Dimensional Boundary Layers, II: Three-Dimensional Flows in Cartesian Coordinates," *AIAA Journal*, Vol. 13, to be published.

[5] Cebeci, T. and Mosinskis, G. J., "Computation of Incompressible Turbulent Boundary Layers at Low Reynolds Numbers," *AIAA Journal*, Vol. 9, Aug. 1971, pp. 1632–1634.

[6] Cebeci, T., "Kinematic Eddy Viscosity at Low Reynolds Numbers," *AIAA Journal*, Vol. 11, Jan. 1973, pp. 102–104.

[7] Bushnell, D. M. and Alston, D. W., "Calculation of Transitional Boundary-Layer Flows," *AIAA Journal*, Vol. 11, April 1973, pp. 554–556.

[8] Cebeci, T., "Wall Curvature and Transition Effects in Turbulent Boundary Layers," *AIAA Journal*, Vol. 9, Sept. 1971, pp. 1868–1870.

[9] Keller, H. B., "A New Difference Scheme for Parabolic Problems," in *Numerical Solution of Partial Differential Equations*, edited by J. Branble, Vol. II, Academic Press, New York, 1970.

[10] Cooper, P., "Turbulent Boundary Layer on a Rotating Disk Calculated with an Effective Viscosity," *AIAA Journal*, Vol. 9, Feb. 1971, pp. 255–261.

[11] Erian, F. F. and Tong, Y. H., "Turbulent Flow due to a Rotating Disk," *Physics of Fluids*, Vol. 14, Dec. 1971, p. 2588.

Elastic Stability of Annular Plates under Uniform Compressive Forces along the Outer Edge

G. K. RAMAIAH* AND K. VIJAYAKUMAR†
Indian Institute of Science, Bangalore, India

I. Introduction

SEVERAL investigations on the problem of elastic stability of annular plates subjected to uniform radial pressure along the outer edge have been reported in the literature.[1–5] Most of these investigations are confined to plates with a free inner edge and clamped or simply supported outer edge. In the present Note, the title problem is analyzed in detail for all nine combinations of clamped, simply supported, and free-edge conditions. The analysis is carried out by the classical Rayleigh-Ritz method with simple polynomials as admissible functions. For annuli of narrow width, suitable coordinate transformations proposed earlier[6,7] are incorporated so as to improve the conditioning of the equations.

II. Analysis

A thin annular plate of constant thickness h, with a and b as the radii of inner and outer edges, respectively, and subjected to uniform inplane radial pressure p_o along the outer edge is considered. Assuming that the plate buckles in n circumferential waves, the lateral deflection $W(r, \theta)$ is expressed as

$$W(r,\theta) = W_n(r)\cos(n\theta+\varepsilon) \tag{1}$$

The strain energy V of bending and the potential T due to midplane forces during bending of the plate are then given by

$$V = \frac{\pi}{2}(1+\delta_{on})D\int_a^b\left[\left(\frac{d^2W_n}{dr^2}+\frac{1}{r}\frac{dW_n}{dr}-\frac{n^2}{r^2}W_n\right)^2 - 2(1-\nu)\frac{d^2W_n}{dr^2}\left(\frac{1}{r}\frac{dW_n}{dr}-\frac{n^2}{r^2}W_n\right) + 2(1-\nu)\frac{n^2}{r^2}\left(\frac{dW_n}{dr}-\frac{W_n}{r}\right)^2\right]r\,dr \tag{2}$$

and

$$T = \frac{\pi}{2}(1+\delta_{on})h\left[\int_a^b\left\{\sigma_r\left(\frac{dW_n}{dr}\right)^2+\sigma_\theta\left(\frac{n}{r}W_n\right)^2\right\}r\,dr\right] \tag{3}$$

in which $\delta_{oo} = 1$ and $\delta_{on} = 0$ for $n \neq 0$, ν is the Poisson's ratio, $D = Eh^3/12(1-\nu^2)$ is the flexural rigidity of the plate, and

$$\sigma_r = -\frac{p_o b^2}{b^2-a^2}\left(1-\frac{a^2}{r^2}\right) \tag{4}$$

Table 1 Transformations

n	First transformation	Second transformation
0	$W_o(r) = w(r)$	$y = (r^2-a^2)/(b^2-a^2)$
1	$W_1(r) = rw(r)$	$y = (r-a)/(b-a)$
$\geqq 2$	$W_n(r) = r^2w(r)$	$y = (r-a)/(b-a)$

$$\sigma_\theta = -\frac{p_o b^2}{b^2-a^2}\left(1+\frac{a^2}{r^2}\right) \tag{5}$$

are the prebuckling membrane stresses.

Following the usual steps in the application of the Rayleigh-Ritz method, the total potential $V+T$ is minimized to obtain relevant characteristic equations for determination of buckling loads. Admissible functions used in the method are chosen to be simple polynomials in r.[6] This procedure, however, is known[6,7] to lead to an ill-conditioned set of equations for annuli of narrow width, particularly in the case of both edges clamped. To overcome this difficulty in computational work, the quantities V and T are expressed, as in earlier analyses,[6,7] in more convenient forms by means of the transformations in Table 1. After obtaining these new expressions for V and T, the Rayleigh-Ritz method is applied with simple polynomials in y as admissible functions.[6] Unlike in the direct analysis, the conditioning of the equations derived thus is found to improve with increasing hole size.

III. Numerical Results and Conclusions

Extensive data for buckling loads are obtained by using direct analysis for $a/b \leqq 0.3$ and by modified analysis for $a/b > 0.3$. In all calculations, the Poisson's ratio $\nu = 0.3$ is used. In view of

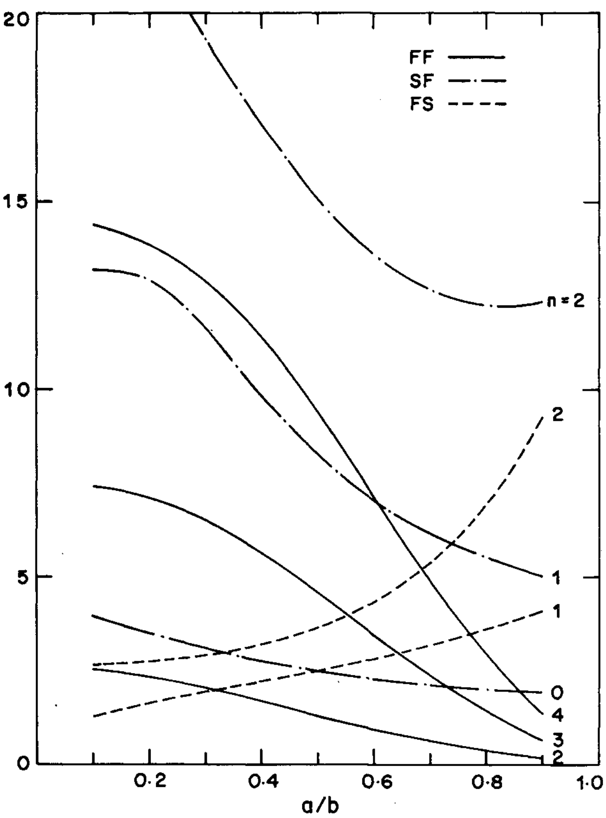

Fig. 1 Variation of buckling load parameter with hole size; —— both edges free (FF), —·— outer edge simply supported and inner edge free (SF), ---- outer edge free and inner edge simply supported (FS). The buckling loads for $n = 0$ are identical in these three cases.[8]

Received October 7, 1974; revision received November 14, 1974.
Index category: Structural Stability Analysis.

* CSIR Research Fellow, Department of Aeronautical Engineering.
† Assistant Professor, Department of Aeronautical Engineering.